

# SU(2) Yang-Mills thermodynamics and photon physics

**R Hofmann**

Institut für Theoretische Physik, Universität Karlsruhe (TH), Kaiserstr. 12,  
76131 Karlsruhe, Germany

E-mail: [hofmann@particle.uni-karlsruhe.de](mailto:hofmann@particle.uni-karlsruhe.de)

## **Abstract.**

Based on quantitative predictions enabled by a nonperturbative approach to Yang-Mills thermodynamics it is explained why the physics of photon *propagation* is not unlikely rooted in pure SU(2) gauge dynamics.

PACS numbers: 70S15;74A15

*Keywords:* thermal ground state, screening, photon polarization, Planck-scale axion  
*Submitted to:* *J. Phys. A: Math. Gen.*

## **1. Introduction**

Physics is the endeavor to understand in mathematical terms the fundamental laws governing our Universe. Quite generally, genuine progress in learning depends on the sophistication and perseverance in posing relevant questions. In physics the content of a question – a prediction – is mathematically deduced from a prejudice (principle, postulate), and the prediction is either verified or falsified by experiment. The more experimentally verified, independent predictions there emerge without any falsification the more truth and generality is attributed to the starting principle.

The purpose of this talk is to discuss implications of the postulate that the physics of photon propagation, which conventionally is associated with a U(1) gauge symmetry, is actually SU(2) Yang-Mills dynamics. While this may seem questionable and contrived judging by a counting of the perturbative degrees of freedom and their universal interactions a thermodynamic approach to SU(2) Yang-Mills theory clearly suggests otherwise [1, 2, 3]. Namely, in the deconfining phase the gauge symmetry SU(2) is broken dynamically down to the subgroup U(1) by a nontrivial thermal ground state. The latter emerges upon a spatial coarse-graining over interacting calorons and anticalorons of topological charge modulus  $|Q| = 1$  [4]. While the thermal ground

state is responsible for the emergence of the (temperature-dependent) mass for two out of the three species of gluons, that is, the dynamical gauge-symmetry breaking  $SU(2) \rightarrow U(1)$ , it also provides for a scale of maximal resolution  $|\phi|$ . The latter uniquely is determined by temperature and the Yang-Mills scale and enforces in the effective theory a rapidly converging loop expansion of thermodynamic quantities. As a consequence, the polarization tensor for the massless mode [2], computed on the one-loop level yields a numerically reliable result for the modification of the dispersion law, and contact with observation and experiment can be made once the above postulate is agreed upon.

This presentation is organized as follows. In Sec.2 we give a brief summary of deconfining and preconfining Yang-Mills thermodynamics. The peculiarities of thermalized photon propagation in light of the above postulate are discussed in Sec. 3. In Sec. 4 we argue for a certain amount of experimental evidence, and in Sec. 5 we provide for an outlook on future activity.

## 2. Deconfining and preconfining $SU(2)$ Yang-Mills thermodynamics

$SU(2)$  Yang-Mills theory takes place in three distinct phases. At high temperature  $T$  (deconfining phase) one shows [4, 5, 6] that an inert (nonfluctuating), adjoint scalar field  $\phi$  emerges upon a spatial coarse-graining over interacting calorons and anticalorons of topological charge modulus  $|Q| = 1$ . Performing this coarse-graining over a trivial-holonomy caloron-anticaloron pair in singular gauge and resorting to a particular global gauge choice, one has

$$\phi = 2 \sqrt{\frac{\Lambda^3 \beta}{2\pi}} t_1 \exp\left(\pm \frac{4\pi i}{\beta} t_3 \tau\right), \quad (1)$$

where  $\Lambda$  is a purely nonperturbative constant of integration (the Yang-Mills scale) [7],  $0 \leq \tau \leq \beta \equiv \frac{1}{T}$  is the euclidean time, and  $t_a$  are  $SU(2)$  generators in the fundamental representation normalized as  $\text{tr} t_a t_b = \frac{1}{2} \delta_{ab}$ . The entire effective action (including the coarse-grained sector of topologically trivial field configurations) follows from perturbative renormalizability [8] and gauge invariance, and the thermal ground state is given by Eq. (1) and the pure-gauge configuration  $a_\mu^{\text{bg}} = \mp \delta_{\mu 4} \frac{2\pi}{e\beta} t_3$ . Here  $e$  is the effective gauge coupling whose evolution with temperature is determined by the Legendre transformations in the effective theory. This evolution possesses an attractor: Evolving downward in temperature,  $e$  rapidly approaches the plateau  $e = \sqrt{8}\pi$  for  $\lambda \equiv \frac{2\pi T}{\Lambda} \gg \lambda_c = 13.87$  and runs into a pole of the form  $e \propto -\log(\lambda - \lambda_c)$ . Here  $T_c$  is the temperature where totally screened magnetic monopoles start to condense. The ground-state pressure  $P^{\text{gs}}$  is negative:  $P^{\text{gs}} = -4\pi\Lambda^3 T$ . By an admissible change of gauge, such that  $\phi \equiv 2 \sqrt{\frac{\Lambda^3 \beta}{2\pi}} t_3$  and  $a_\mu^{\text{bg}} = 0$ , the adjoint Higgs mechanism manifestly generates quasiparticle masses for the topologically trivial gauge fields  $a_\mu^{1,2}$  while the field  $a_\mu^3$  remains massless. Radiative corrections to thermodynamic quantities are small even though the plateau value of  $e$  is not small. They are computed in a loop expansion in the effective theory [9]. This expansion converges rapidly because of infrared stability enabled by quasiparticle masses on tree level and because of kinematic constraints due

to the existence of the maximal resolution  $|\phi|$ . In particular, it is sufficient for practical purposes to compute the polarization tensor of the massless mode to one-loop accuracy only [2]. Depending on their frequency, there is screening or antiscreening in a thermal gas of massless particles due to scattering involving the massive modes. Because of the dynamical gauge symmetry breakdown  $SU(2) \rightarrow U(1)$  it is tempting to attribute the existence and propagation of the photon to this Yang-Mills theory. In the preconfining phase, that is, for  $T$  slightly below  $T_c$  magnetic‡ monopoles start to condense. In spatial regions, where a stable condensate prevails, the unbroken  $U(1)$  symmetry of the deconfining phase is dynamically broken. For the photon this would mean that an additional polarization emerges if temperature falls below  $T_{\text{CMB}}$ .

Because no screening or antiscreening is observed for long-wavelengths photons emitted by astrophysical sources and propagating towards Earth above the present ground state of the cosmic microwave background (CMB) and because this is the situation predicted at  $T_c$  by an  $SU(2)$  Yang-Mills theory§ we are led to identify  $T_c$  with the present value of  $T_{\text{CMB}} \sim 2.73 \text{ K}$ . This, in turn, fixes the Yang-Mills scale as  $\Lambda_{\text{CMB}} = 2.35 \times 10^{-4} \text{ eV}$ .

### 3. The postulate $SU(2)_{\text{CMB}} \stackrel{\text{today}}{=} U(1)_{\text{photon}}$

Subjecting photon propagation to an  $SU(2)$  gauge principle we refer to the two massive modes as  $V^\pm$  and, as usual, to the massless excitation as  $\gamma$ . Screening or antiscreening of thermalized  $\gamma$ -radiation is a small effect for thermodynamic quantities such as the pressure [2] which peaks at about twice  $T_c$ . Depending on its frequency  $\omega$  and spatial momentum  $\vec{p}$ , the modification of the  $U(1)$  dispersion law is as

$$\omega^2 = \vec{p}^2 \longrightarrow \omega^2 = \vec{p}^2 + G(\omega, |\vec{p}|, T, \Lambda_{\text{CMB}}). \quad (2)$$

The function  $G$  enters the polarization tensor  $\Pi_{\mu\nu}$ . For  $\omega = |\vec{p}|$  the function  $G$  is real, corresponds to  $\Pi_{11} = \Pi_{22}$  if  $\vec{p}$  points into the 3-direction, and is computed according|| to the Feynman diagram B in Fig. 1. In Fig. 2 the dependence of  $G$  on dimensionless momentum  $X \equiv \frac{|\vec{p}|}{T}$  is depicted for various temperatures¶. To the left (right) of the cusps  $G$  is positive (negative) corresponding to screening (antiscreening). Points lying above the dashed curve are associated with strongly screened modes (screening mass larger than modulus of momentum).

What are the implication of the modification in Eq.(2) for the black-body spectrum? The total energy density  $\rho$  of a thermal gas of  $\gamma$  is defined as

$$\rho \equiv 2 \int \frac{d^3p}{(2\pi)^3} \omega n_B \left( \frac{\omega}{T} \right), \quad (3)$$

‡ Magnetic w.r.t. the defining  $SU(2)$  Yang-Mills theory, electric w.r.t. photons.

§ At  $T_c$  massive quasiparticles decouple thermodynamically and thus do not contribute to screening or antiscreening of the massless mode [2, 3, 10].

|| If the condition  $\omega = |\vec{p}|$  is sizably modified then also Feynman diagram A in in Fig. 1 contributes, and  $G$  acquires an imaginary part.

¶ Setting  $\omega = |\vec{p}|$  in  $G$  makes it a function of  $\omega$  only. This approximation turns out to be selfconsistent [3] for almost all values of  $\omega$ .

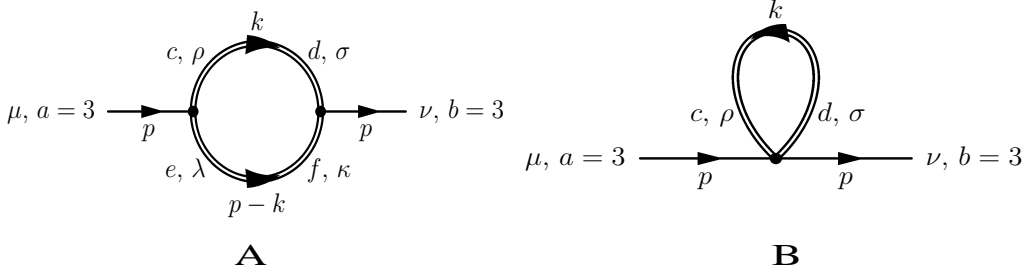


**Figure 1.** The diagrams for the TLM mode polarization tensor.

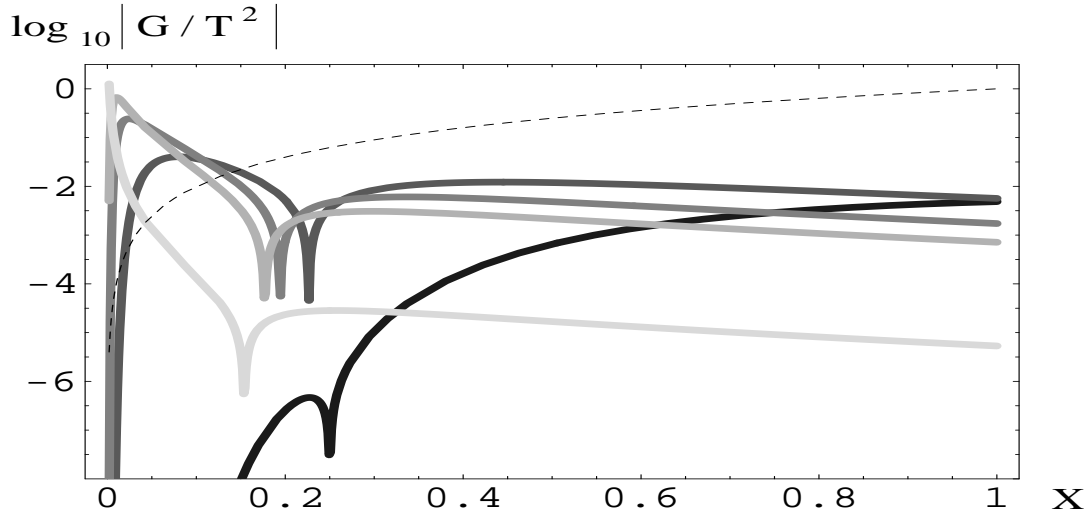


**Figure 2.** A plot of  $\log_{10} \frac{|G|}{T^2}$  as a function of  $X$  for  $\lambda = 1.12 \lambda_c$  (black),  $\lambda = 2 \lambda_c$  (dark grey),  $\lambda = 3 \lambda_c$  (grey),  $\lambda = 4 \lambda_c$  (light grey),  $\lambda = 20 \lambda_c$  (very light grey). The dashed curve depicts the function  $f(X) = 2 \log_{10} X$ .

where  $n_B(x) \equiv \frac{1}{\exp[x]-1}$  denotes the Bose distribution. Expressing the momentum-space measure  $d^3p$  in terms of a frequency measure under consideration of the modified dispersion law in Eq. (2), one has

$$\int d^3p = 4\pi \int d|\vec{p}| |\vec{p}|^2 = 4\pi \int d\omega \sqrt{\omega^2 - G(\omega)} \left( \omega - \frac{1}{2} \frac{dG(\omega)}{d\omega} \right), \quad (4)$$

where the additional dependence of  $G$  on  $T$  is suppressed. In the strong-screening regime the quantity  $|\vec{p}|$  would be imaginary, and thus the integration over  $\omega$  is restricted to a domain where  $\omega^2 \geq G$ . Thus we can write the spectral intensity  $I_{\text{SU}(2)}(\omega)$  of the SU(2)-modified black body in terms of the spectral intensity  $I_{\text{U}(1)}(\omega)$  of the U(1) black body as

$$I_{\text{U}(1)}(\omega) \rightarrow I_{\text{SU}(2)}(\omega) = I_{\text{U}(1)}(\omega) \times \frac{\left( \omega - \frac{1}{2} \frac{d}{d\omega} G \right) \sqrt{\omega^2 - G}}{\omega^2} \theta(\omega - \omega^*), \quad (5)$$

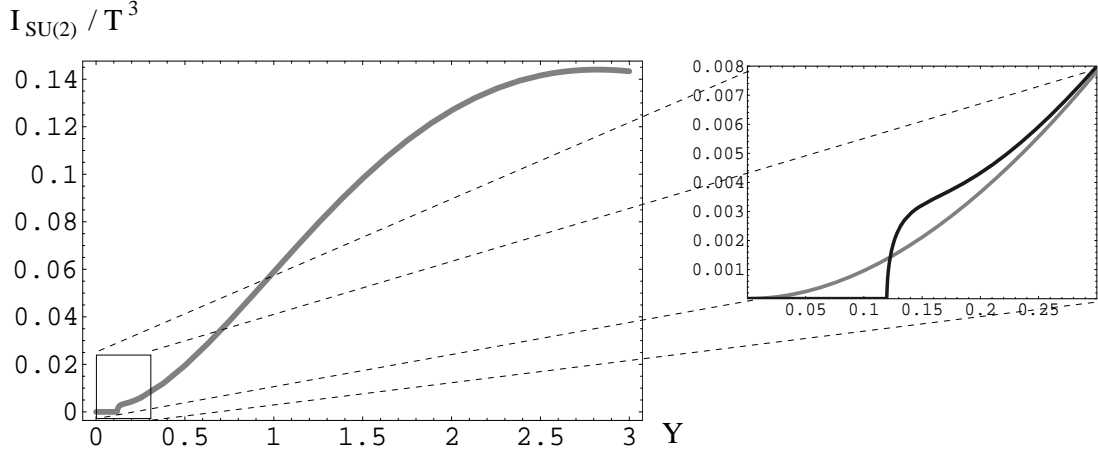


**Figure 3.** Dimensionless black-body spectral power  $\frac{I_{\text{SU}(2)}}{T^3}$  as a function of the dimensionless frequency  $Y \equiv \frac{\omega}{T}$ . The black curve in the magnified region depicts the modification of the spectrum as compared to  $\frac{I_{\text{U}(1)}}{T^3}$  (grey curve) for  $T = 10$  K.

where  $\omega^*$  is the root<sup>+</sup> of  $\omega^2 = G$ ,  $\theta(x)$  is the Heaviside step function, and

$$I_{\text{U}(1)}(\omega) = \frac{1}{\pi^2} \frac{\omega^3}{\exp[\frac{\omega}{T}] - 1}. \quad (6)$$

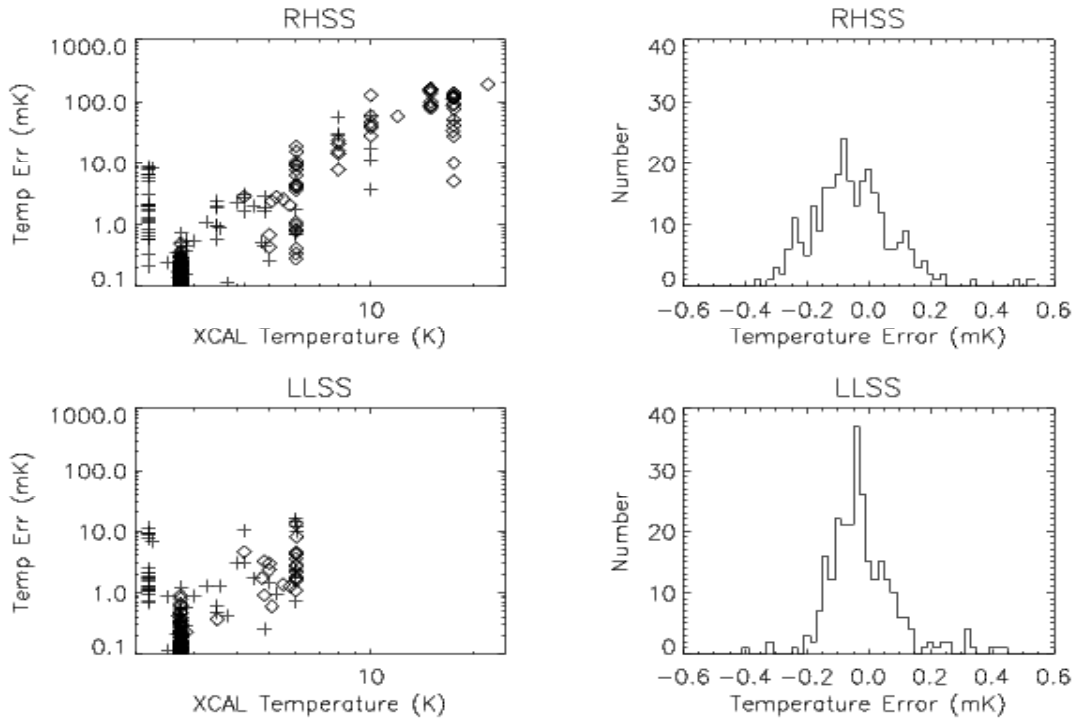
Fig. 3 depicts the modified black-body spectrum according to Eq. (5) at  $T = 10$  K. For  $T < T_c = T_{\text{CMB}}$   $\gamma$  starts to acquire a Meissner mass, and the average number of photon polarizations rapidly increases from two towards three. This, in turn, implies a rapid increase of the energy density of the photon gas as compared to its value in the U(1) theory.

#### 4. Evidence in nature?

In [12] an analysis of the predictions of  $\text{SU}(2)_{\text{CMB}}$  for temperature offsets\*  $\delta T$  was performed along the lines of the COBE Firas situation. Their data of the spectral shape of the black-body intensity for temperatures in the vicinity of  $T_{\text{CMB}} = 2.73$  K was taken during the calibration stage of the instrument [11]. A comparison of their temperature offsets  $\delta T$  with the predictions of  $\text{SU}(2)_{\text{CMB}}$  reveals that the predicted anomaly is smaller than the experimental error in the FIRAS calibration. What is interesting, however, is the sudden increase of  $\delta T$  for  $T_{\text{XCAL}} < T_{\text{CMB}}$ , see Fig. 4, which we attribute to an increase of the average number of photon polarizations at the onset of the preconfining phase, for a discussion see [12]. Next there is large-angle suppression in the CMB TT power spectrum and the statistical correlation of the low multipoles [13]. Based on the black-body anomaly predicted by  $\text{SU}(2)_{\text{CMB}}$  a model for the generation of large-angle temperature fluctuations in the CMB was proposed in [14] which has the potential to explain these effect in terms of a large dynamical contribution to the CMB

<sup>+</sup> There are actually two roots, compare with Fig. 2. For many practical concerns the lower lying root can safely be set equal to zero.

\* Defined by  $\delta T \equiv T_{\text{rad}} - T_{\text{XCAL}}$ , where  $T_{\text{rad}}$  is extracted by fitting  $I_{\text{U}(1)}$  to the intensity of the radiation and  $T_{\text{XCAL}}$  is the (wall) temperature of the calibrator.



Photometric XCAL temperature adjustments — The values for RHSS (top plots) and LLSS (bottom plots) calibrations are shown here. The left hand plots are the adjustments (in mK), plotted as a function of XCAL temperature (in K). The symbol + indicates a positive correction, and the symbol  $\diamond$  indicates a negative correction. Temperatures greater than 7K are not used in LLSS. On the right are histograms of temperature adjustments for cold nulls (i.e. all controllables  $\sim 2.7$ K).

**Figure 4.** Temperature offsets as measured in the FIRAS orbit calibration. Notice the peak at  $T = 2.2$  K. Figure taken from [11].

dipole, see also [12]. Third, large, old, cold, and dilute clouds of atomic hydrogen were discovered in between spiral arms of the outer Milky Way, see [15]. The puzzling fact about these clouds is their inferred age of about 50 million years. This is much older than model calculations for the duration for the formation of sizable fractions of  $H_2$  molecules suggest, for one of the newer investigations see [16]. In [3] it was pointed out that the interatomic distance of about 1 cm between the hydrogen atoms is roughly equal to the wavelength of screened photons at the relevant (brightness) temperatures of 5 K to 10 K, and that the 21 cm–line, which thermalizes the cloud system, propagates. By computing the two-point correlator of the photon energy density, this observation is confirmed [17]. That is, photons, needed to mediate interactions between the hydrogen atoms, are screened due to the nonabelian effects of  $SU(2)_{\text{CMB}}$ , and the cloud changes its composition on a much slower rate than conventionally expected. Fourth, a scenario was discussed in [18] where the nontrivial thermal ground state of  $SU(2)_{\text{CMB}}$ , by virtue of dynamical chiral symmetry breaking [19] and the chiral anomaly [20] invoked at the Planck scale, gives rise to an ultralight axion field. If CP violating signatures, such as a nonvanishing EB cross correlation at large angles, will be discovered in future CMB satellite missions, then this Planck-scale axion field would yield a theoretically and observationally backed up explanation of the present cosmological concordance model. That is, the physics of visibility (propagating photons) would be unified with the physics

of darkness (dark matter and dark energy) in terms of an SU(2) gauge principle.

Finally, let us discuss an apparent puzzle: Even at room temperature a sizable fraction of the radiowave spectrum is screened according to the modified dispersion law in Eq.(2). But we do not observe this screening in our daily broadcasts. So why is this? The answer is that the intensity in a beam of radiowaves of a given frequency, as transmitted by a commonly used antenna, is by orders of magnitude larger than its corresponding black-body intensity. Thus those radiowaves are a priori not part of the thermal black-body spectrum at, say, room temperature. The question then arises how long it takes for radiowaves to decrease their energy by radiating off  $V^\pm$  particles to eventually be part of the thermal spectrum. The rate for this process is determined by the imaginary part of a two-loop diagram (involving two four-vertices) for the polarization tensor. Since the real part of a two-loop diagram generally is suppressed by a factor of  $\sim 10^{-3}$  [2] as compared to the one-loop result and since there is an even greater suppression for the imaginary part we expect no adulteration of radiowave propagate over terrestrial distances as compared to the U(1) theory. Recall, that there is no screening effect or energy loss whatsoever for photon propagation above the present CMB ground state (radiowave propagation in space) due to the thermal decoupling of  $V^\pm$  at  $T_c = T_{\text{CMB}} = 2.73$  K.

## 5. Conclusions and outlook

In this talk we have given a brief account of why deconfining SU(2) Yang-Mills thermodynamics may be the theory underlying photon propagation. We have mentioned evidence in favor of this postulate. A conclusive judgement will, however, be provided by a direct terrestrial measurement of the spectral intensity of a low-temperature (say,  $T = 5$  K to  $T = 10$  K) black body at low frequencies. If the spectral gap, as predicted by  $\text{SU}(2)_{\text{CMB}}$ , indeed is seen in a precision black-body experiment then this would imply far-reaching consequences for our understanding of electroweak symmetry breaking, for a discussion see [3].

Some of our future activity will be focussing on predictions of the average number of photon polarizations in the supercooled, finite-volume situation.

## References

- [1] R. Hofmann, PoS JHW2005, **021** (2006) [hep-ph/0508176].
- [2] M. Schwarz, R. Hofmann, and F. Giacosa, Int. J. Mod. Phys. A **22**, 1213 (2007) [hep-th/0603078].
- [3] M. Schwarz, R. Hofmann, and F. Giacosa, JHEP **0702**, 091 (2007) [hep-ph/0603174].
- [4] R. Hofmann, Int. J. Mod. Phys. A**20**, 4123 (2005), Erratum-ibid A**21**, 6515 (2006) [hep-th/0504064].
- [5] U. Herbst and R. Hofmann, hep-th/0411214.
- [6] R. Hofmann, arXiv:0710.0962 [hep-th].
- [7] F. Giacosa and R. Hofmann, hep-th/0609172, to appear in Prog. Theor. Phys.
- [8] 't Hooft G., Veltman M. J. G., Nucl. Phys. B**44** (1972) 189.  
't Hooft G., Veltman M. J. G., Nucl. Phys. B**50** (1972) 318.

- 't Hooft G., Nucl. Phys. **B33** (1971) 173.  
't Hooft G., Nucl. Phys. **B62** (1973) 444.
- [9] R. Hofmann, hep-th/0609033.
- [10] U. Herbst, R. Hofmann, J. Rohrer, Acta Phys. Polon. **B36**, 881 (2005) [hep-th/0410187].
- [11] FIRAS Explanatory Supplement, available at <http://lambda.gsfc.nasa.gov/product/cobe/firas-exsupv4.cfm>.
- [12] M. Szopa, R. Hofmann, F. Giacosa, and M. Schwarz, arXiv:0707.3020 [hep-ph].
- [13] C. Copi, D. Huterer, D. Schwarz, and G. Starkman, Phys. Rev. D **75**, 023507 (2007) [astro-ph/0605135].
- [14] M. Szopa and R. Hofmann, hep-ph/0703119.
- [15] L. B. G. Knee and C. M. Brunt, Nature **412**, 308-310 (2001).
- [16] P. Goldsmith, D. Li, and M. Krčo, Astrophys. J. **654**, 273 (2007).
- [17] J. Keller, R. Hofmann, and F. Giacosa, to be published.
- [18] F. Giacosa and R. Hofmann, Eur. Phys. J. **C50**, 635 (2007) [hep-th/0512184].
- [19] T. Banks and A. Casher, Nucl. Phys. B **169**, 103 (1980).
- [20] S. L. Adler, Phys. Rev. **177**, 2426 (1969).  
S. L. Adler and W. A. Bardeen, Phys. Rev. **182**, 1517 (1969).  
J. S. Bell and R. Jackiw, Nuovo Cim. **A60**, 47 (1969).